Supporting Information

Thermochromism and X-ray Detection Capabilities of a Hybrid Double Metal Halide Perovskite $(C_3H_{12}N_2)_2AgBiBr_8$

Kanika Parashar[a], Tamanna Pinky[a], Nobuyuki Yamamoto[a], S. A. Keishana Navodye[b], G.T. Kasun Kalhara Gunasooriya[b], Mark D. Smith[c], Bayram Saparov[a*]

[a]Department of Chemistry & Biochemistry, The University of Oklahoma, Norman, Oklahoma 73019-5251, United States

[b]School of Sustainable Chemical, Biological and Materials Engineering, The University of Oklahoma, Norman, Oklahoma 73019-5251, United States

[c]Department of Chemistry and Biochemistry, University of South Carolina, Columbia, South Carolina 29208, United States

*Author to whom correspondence should be addressed: saparov@ou.edu

Table S1. Selected single crystal data and structure refinement parameters for $(C_3H_{12}N_2)_2AgBiBr_8$ at low temperature (100 K) and high-temperature (400 K).

Formula	**$(C_3H_{12}N_2)_2AgBiBr_8$**	
Formula weight (g/mol)	1108.42	1108.42
Temperature (K)	100(2)	400(2)
Radiation, wavelength (Å)	MoKα (λ = 0.71073)	MoKα (λ = 0.71073)
Crystal system	Monoclinic	Monoclinic
Space group	$P2_1/n$	$C2/m$
Z	2	2
Unit cell parameters (Å)	a = 8.3736(3) b = 7.6960(3) c = 18.2768(7) β = 99.008(10)°	a = 18.9998(15) b = 7.8787(7) c = 8.3765(8) β = 107.287(3)°
Volume (Å^3)	1163.29(8)	1197.27(18)
Density (g/cm^3)	3.164	3.075
Absorption coefficient (μ/mm^{-1})	22.131	21.503
2Θ range for data collection/°	5.086 to 56.654	2.547 to 27.098
Reflections collected	24212	11483
Independent reflections	2902 [R_{int} = 0.0634, R_{sigma} = 0.0373]	1415 [R_{int} = 0.0449]
Final R indexes [I>=2σ (I)]	R_1 = 0.0372 wR_2 = 0.1005	R_1 = 0.0240 wR_2 = 0.0579
Final R indexes [all data]	R_1 = 0.0390 wR_2 = 0.1019	R_1 = 0.0264 wR_2 = 0.0598
Goodness-of-fit on F^2	1.054	1.054
Largest diff. peak and hole (e$^-$/Å^3)	3.34 and -1.53	0.518 and -0.727

$$R_1 = \sum||F_0| - |F_c||/\sum|F_0|; wR_2 = |\Sigma|w(F_0^2 - F_c^2)^2/\sum|wF_0^{22}|_{1/2}$$

where $w = 1/|\sigma^2F_0^2 + (AP)^2 + BP|$, with $P = (F_0^2 + 2F_c^2)/3$ and weight coefficients A and B

Table S2. Fractional atomic coordinates ($\times 10^4$) and equivalent isotropic displacement parameters (U_{eq}[a]) ($Å^2 \times 10^3$) for $(C_3H_{12}N_2)_2AgBiBr_8$ at 100 K.

Atom	*x*	*y*	*z*	U_{eq}
Bi1	5000	5000	0	17.83(12)
Ag1	0	0	0	23.17(16)
Br1	1039.0(7)	167.5(7)	1426.8(3)	23.72(15)
Br2	2223.2(6)	2858.8(7)	-338.1(3)	23.76(15)
Br3	4622.4(7)	5136.9(7)	1525.3(3)	23.03(16)
Br4	7062.2(6)	2075.1(7)	268.9(3)	22.72(15)
N1	619(6)	4454(7)	1234(3)	25.2(9)
N2	6(6)	4622(7)	3639(3)	25.7(10)
C1	549(8)	5152(7)	1986(4)	25.7(12)
C2	-933(6)	4415(7)	2275(3)	22.9(10)
C3	-1209(8)	5223(8)	3003(4)	26.4(12)

[a]U_{eq} is defined as one third of the trace of the orthogonalized U_{ij} tensor.

Table S3. Fractional atomic coordinates ($\times 10^4$) and equivalent isotropic displacement parameters (U_{eq}[a]) ($Å^2 \times 10^3$) for $(C_3H_{12}N_2)_2AgBiBr_8$ at 400 K.

Atom	*x*	*y*	*z*	U_{eq}
Bi1	5000	10000	5000	50(1)
Ag1	5000	5000	0	68(1)
Br1	6419(1)	5000	446(1)	94(1)
Br2	5257(1)	7495(1)	2833(1)	108(1)
Br3	3471(1)	10000	3186(1)	87(1)
N1A	3680(30)	4580(160)	3370(120)	85(7)
N2A	1280(40)	4200(130)	610(90)	78(10)
N1	3689(10)	4770(80)	3690(30)	85(7)
N2	1242(13)	4660(20)	660(30)	78(10)
C1	3028(7)	5270(40)	4187(18)	79(6)
C2	2340(7)	4464(18)	3112(16)	74(4)
C3	2004(8)	5310(30)	1474(16)	86(6)
C1A	3080(20)	5600(80)	3720(50)	78(7)
C2A	2400(20)	5660(50)	2300(50)	75(6)
C3A	1830(20)	4370(60)	2270(50)	89(7)

[a] U_{eq} is defined as one third of the trace of the orthogonalized U_{ij} tensor.

Table S4. Selected bond distances and angles in $(C_3H_{12}N_2)_2AgBiBr_8$ at 100 K.

Atom pair	Distance (Å)	Label	Angle (°)
Bi1 – Br2[1]	2.8379(5)	Br2[1] – Bi1 – Br2	180.0
Bi1 – Br2	2.8379(5)	Br2[1] – Bi1 – Br3[1]	91.251(16)
Bi1 – Br3[1]	2.8562(6)	Br2 – Bi1 – Br3	91.250(16)
Bi1 – Br3	2.8563(6)	Br2[1] – Bi1 – Br3	88.749(16)
Bi1 – Br4[1]	2.8328(5)	Br2 – Bi1 – Br3[1]	88.750(16)
Bi1 – Br4	2.8328(5)	Br3[1] – Bi1 – Br3	180.0
Ag1 – Br1[2]	2.6197(6)	Br4 – Bi1 – Br2	91.879(14)
Ag1 – Br1	2.6198(6)	Br4[1] – Bi1 – Br2[1]	91.879(14)
Ag1 – Br2	3.0080(5)	Br4[1] – Bi1 – Br2	88.121(14)
Ag1 – Br2[2]	3.0081(5)	Br4 – Bi1 – Br2[1]	88.121(14)
Ag1 – Br4[3]	3.0367(5)	Br4[1] – Bi1 – Br3	88.989(15)
Ag1–Br4[4]	3.0367(5)	Br4[2] – Bi1 – Br3[1]	91.010(15)
N1 – C1	1.486(8)	Br4 – Bi1 – Br3[1]	88.991(15)
N2 – C3	1.494(8)	Br4 – Bi1 – Br3	91.009(15)
C1 – C2	1.531(8)	Br4[1] – Bi1 – Br4	180.0
C2 – C3	1.520(8)	Br1[2] – Ag1 – Br1	180.0
		Br1 – Ag1 – Br2	92.795(16)
		Br1[2] – Ag1 – Br2[2]	92.796(16)
		Br1[2] – Ag1 – Br2	87.205(16)
		Br1 – Ag1 – Br2[2]	87.204(16)
		Br1[2] – Ag1 – Br4[3]	87.950(16)
		Br1 – Ag1 – Br4[3]	92.050(16)
		Br1[2] – Ag1 – Br4[4]	92.050(16)
		Br1 – Ag1 – Br4[4]	87.950(16)
		Br2 – Ag1 – Br2[2]	180.0
		Br2[2] – Ag1 – Br4[4]	78.951(14)

Br2 – Ag1 – Br4[4]	101.049(14)
Br2 – Ag1 – Br4[3]	78.951(14)
Br2[2] – Ag1 – Br4[3]	101.049(14)
Br4[3] – Ag1 – Br4[4]	180.00(2)
Bi1 – Br2 – Ag1	153.16(2)
Bi1 – Br4 – Ag1[5]	151.29(2)
N1 – C1 – C2	109.6(5)
C3 – C2 – C1	113.1(5)
N2 – C3 – C2	112.1(5)

Here, [1]1-X, 1-Y, -Z; [2]-X, -Y, -Z; [3]1-X, -Y, -Z; [4]-1+X, +Y, +Z; [5]1+X, +Y, +Z

Table S5. Selected bond distances and angles in $(C_3H_{12}N_2)_2AgBiBr_8$ at 400 K.

Atom pair	Distance (Å)	Label	Angle (°)
Bi1 – $Br2^4$	2.8204(5)	Br2 – Bi1 – $Br2^6$	180.00(3)
Bi1 – Br2	2.8204(5)	Br2 – Bi1 – $Br2^5$	88.80(4)
Bi1 – $Br2^6$	2.8204(5)	$Br2^4$ –Bi1– $Br2^6$	88.80(4)
Bi1 – $Br2^5$	2.8204(5)	$Br2^4$-Bi1-$Br2^5$	180.0
Bi1 – Br3	2.8501(8)	$Br2^4$-Bi1-$Br3^6$	90.03(2)
Bi1 – $Br3^6$	2.8502(8)	$Br2^4$-Bi1-Br3	89.97(2)
Ag1 – $Br2^1$	3.0075(6)	$Br2^6$-Bi1-Br3	89.97(2)
Ag1 – Br1	2.6101(8)	Br2-Bi1-$Br3^6$	89.97(2)
Ag1 – Br2	3.0075(6)	Bi1-Br2-Ag1	161.20(3)
Ag1 – $Br2^3$	3.0075(6)	$Br2^6$-Bi1-$Br2^5$	91.20(4)
Ag1 – $Br2^2$	3.0075(6)	Br2-Bi1-$Br2^4$	91.20(4)
Ag1–$Br1^1$	3.0075(6)	Br2-Bi1-Br3	90.03(2)
N1 – C1	1.488(19)	$Br2^5$-Bi1-$Br3^6$	89.97(2)
N2 – C3	1.50(2)	$Br2^6$-Bi1-$Br3^6$	90.03(2)
C1 – C2	1.491(15)	$Br2^5$-Bi1-Br3	90.03(2)
C2 – C3	1.487(15)	Br3-Bi1-$Br3^6$	180.0
		$Br1^1$-Ag1-Br1	180.0
		Br1-Ag1-$Br2^3$	88.20(2)
		Br1-Ag1-Br2	88.21(2)
		$Br1^1$-Ag1-$Br2^1$	88.20(2)
		Br1-Ag1-$Br2^2$	91.80(2)
		$Br2^1$-Ag1-$Br2^2$	81.64(3)
		$Br2^1$-Ag1-$Br2^3$	98.36(3)
		$Br2^2$-Ag1-Br2	98.36(3)
		$Br1^1$-Ag1-$Br2^2$	88.20(2)
		$Br1^1$-Ag1-Br2	91.79(2)

Br1-Ag1-Br2[1]	91.80(2)
Br1[1]-Ag1-Br2[3]	91.80(2)
Br2[3]-Ag1-Br2[2]	180.00(3)
Br2[3]-Ag1-Br2	81.64(3)
Br2[1]-Ag1-Br2	180.0
C2 – C3 – N2	111.0(16)
N1 – C1 – C2	112.4(18)
C3 – C2 – C1	115.3(14)

Here, [1]-X+1, -Y+1, -Z; [2]-X+1, Y, -Z; [3]X, -Y+1, Z; [4]-X+1, Y, -Z+1; [5]X, -Y+2, Z; [6]-X+1, -Y+2, -Z+1

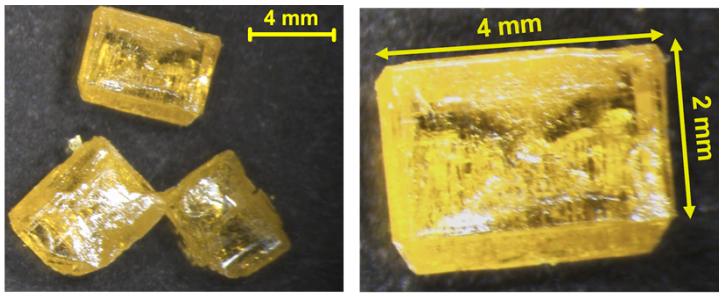

Fig. S1 Images of $(C_3H_{12}N_2)_2AgBiBr_8$ crystals synthesized using the slow evaporation growth method.

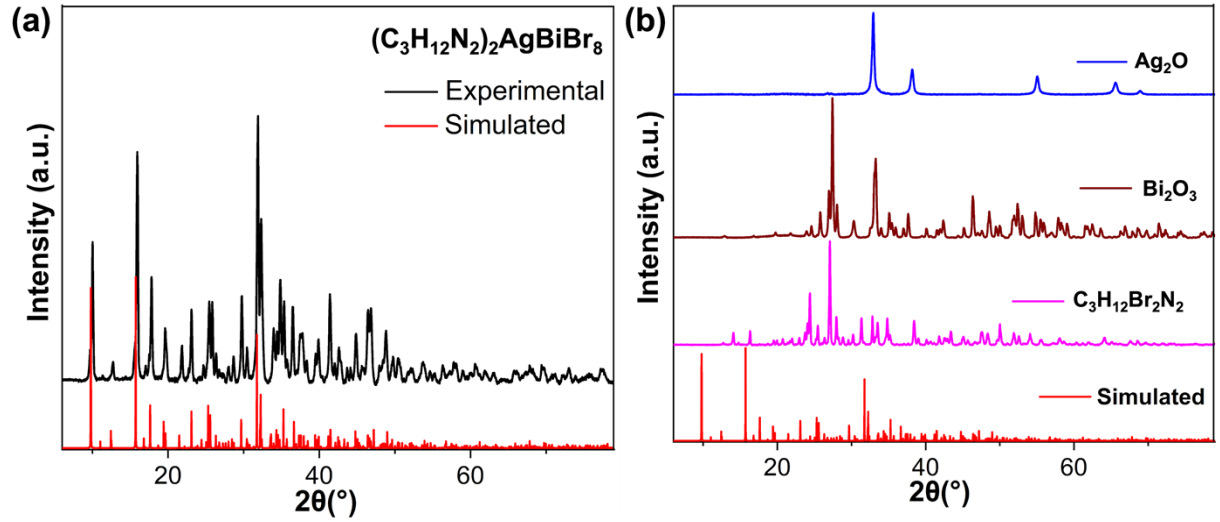

Fig. S2 Comparison of simulated diffraction data (in red) of $(C_3H_{12}N_2)_2AgBiBr_8$ with its (a) room temperature PXRD pattern (in black). (b) $(C_3H_{12}N_2)_2AgBiBr_8$ is obtained as a phase pure sample no Ag_2O (blue), Bi_2O_3 (wine), and $C_3H_{12}Br_2N_2$ (pink) impurities are detected.

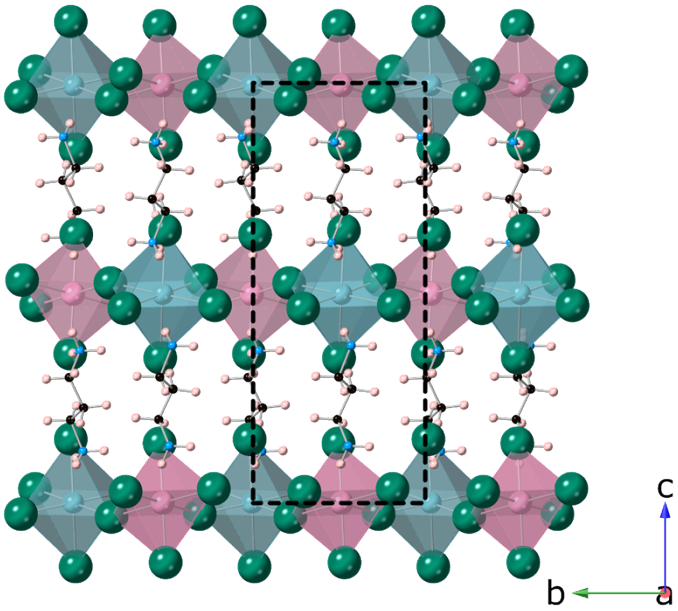

Fig. S3 Layered crystal structure of $(C_3H_{12}N_2)_2AgBiBr_8$ is depicted. Silver, bismuth, bromine, nitrogen, carbon and hydrogen are represented by pink, bluish-green, green, blue, black and peach spheres, respectively.

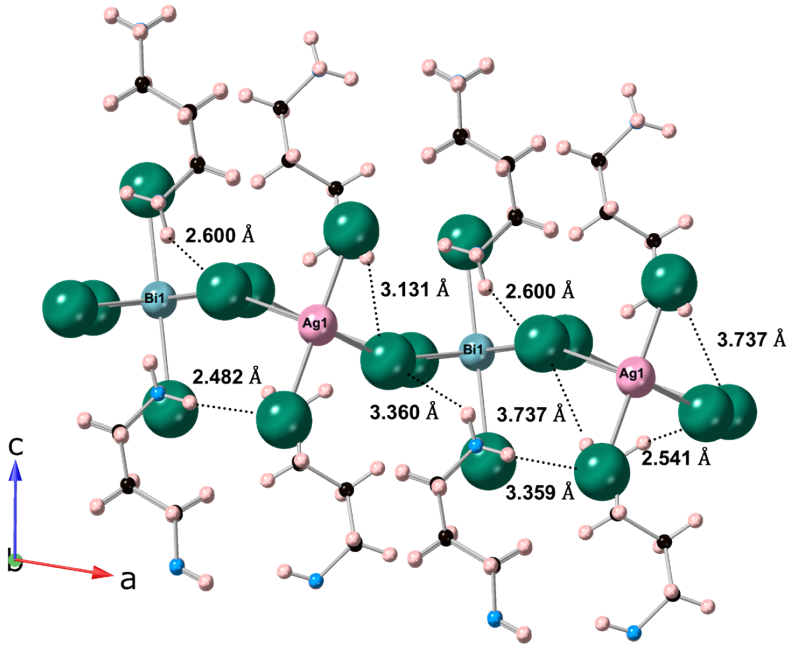

Fig. S4 Hydrogen bonding network between a 2D $[AgBiBr_8]^{4-}$ layer and intervening $[C_3H_{12}N_2]^{2+}$ cations within the crystal structure of $(C_3H_{12}N_2)_2AgBiBr_8$ is depicted. Silver, bismuth, bromine, nitrogen, carbon, and hydrogen are denoted by pink, bluish-green, green, blue, black and peach spheres, respectively.

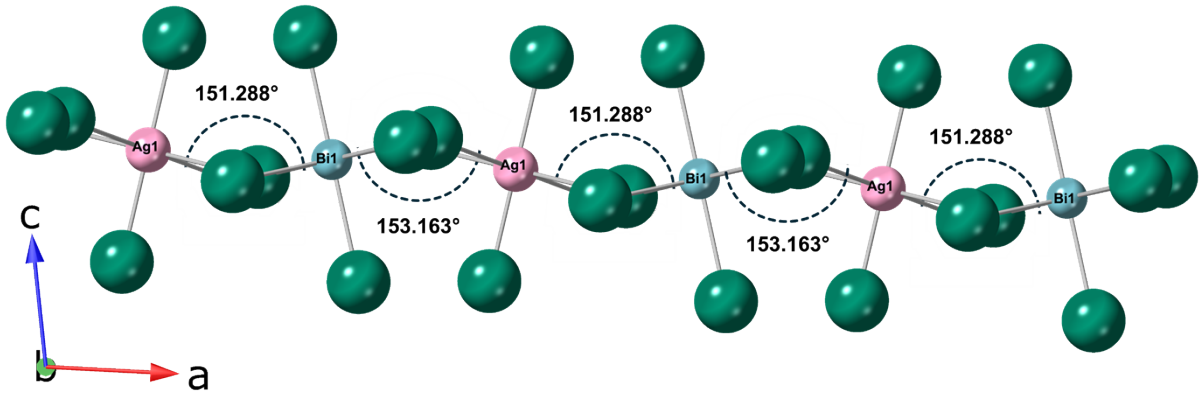

Fig. S5 The bridging Ag-Br-Bi and Bi-Br-Ag angles within the inorganic layers the in-plane direction shows considerable tilting. Silver, bismuth and bromine are denoted by pink, bluish-green and green spheres, respectively.

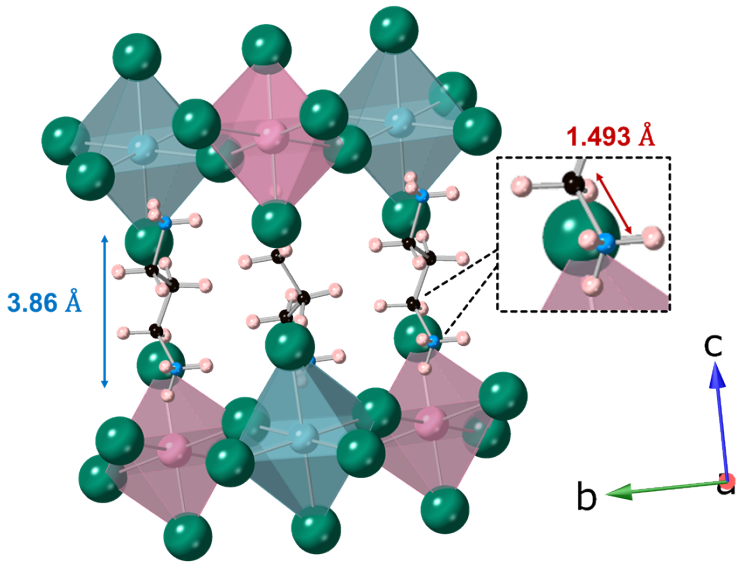

Fig. S6 Interlayer spacing and penetration depth of the organic cations in $(C_3H_{12}N_2)_2AgBiBr_8$. Silver, bismuth, bromine, nitrogen, carbon, and hydrogen are denoted by pink, bluish-green, green, blue, black and peach spheres, respectively.

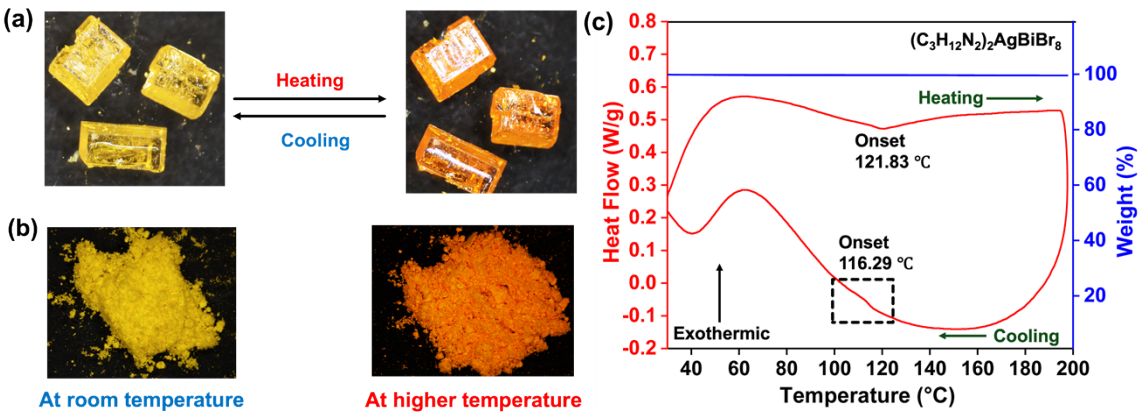

Fig. S7 $(C_3H_{12}N_2)_2AgBiBr_8$ sample shows reversible color changes during heating-cooling cycles: (a) single crystals and (b) polycrystalline powders. (c) Thermogravimetric Analysis (TGA, blue) and Differential Scanning Calorimetry (DSC, red) curves from 30℃ to 200℃.

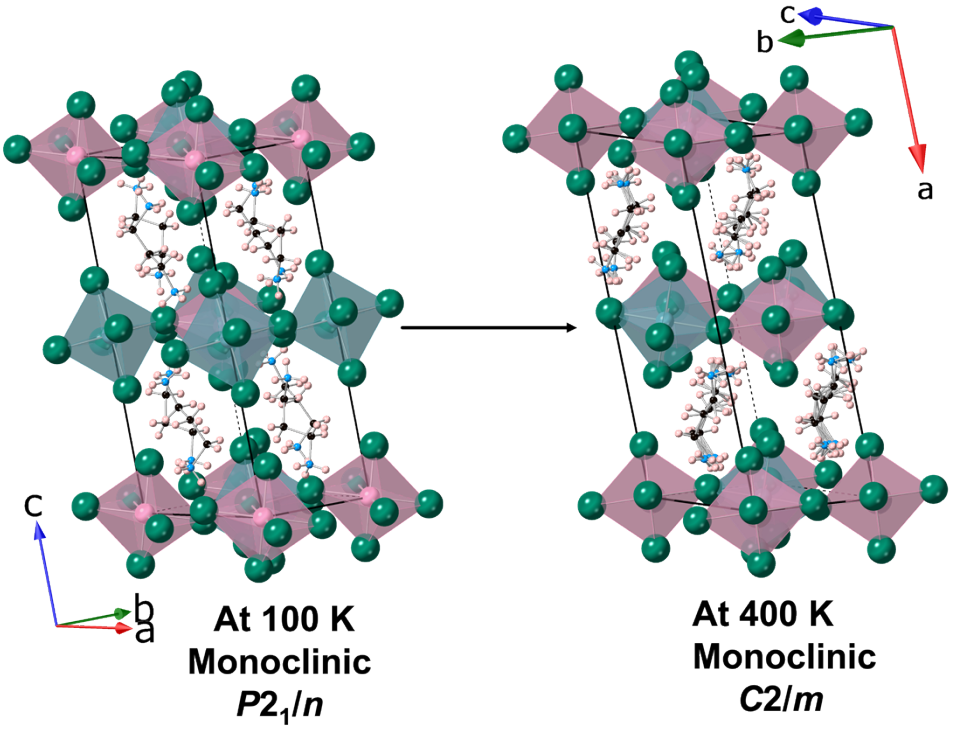

Fig. S8 Crystal structures of $(C_3H_{12}N_2)_2AgBiBr_8$ below (100 K) and above (400 K) the transition temperature. Silver, bismuth, bromine, nitrogen, carbon and hydrogen are represented by pink, bluish-green, green, blue, black and peach spheres, respectively.

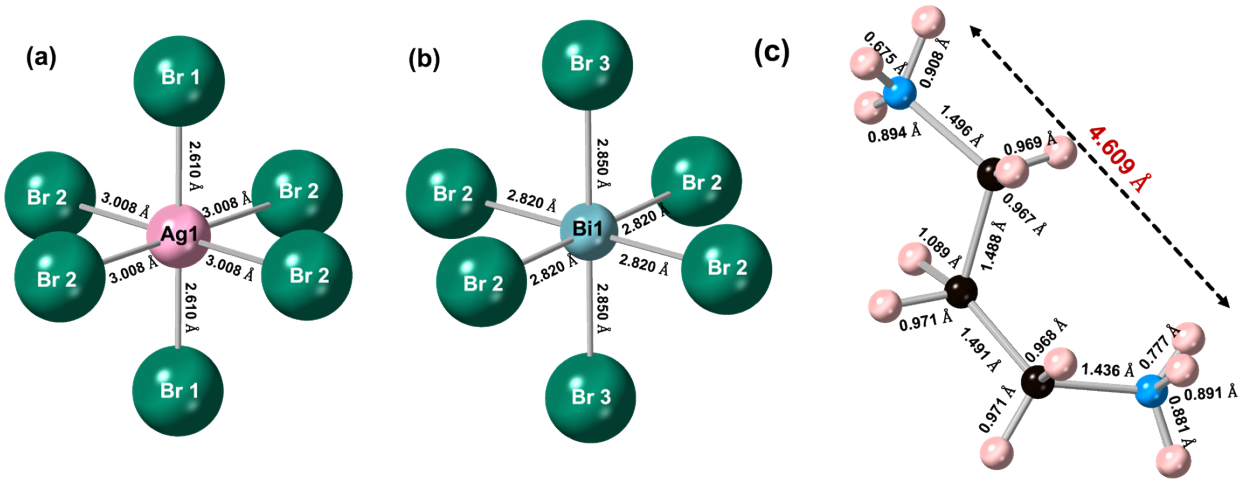

Fig. S9 Interatomic distances in the coordination environments of (a) silver and (b) bismuth, and (c) in the organic $C_3H_{12}N_2^{2+}$ cation at 400 K. Silver, bismuth, bromine, nitrogen, carbon and hydrogen are represented by pink, bluish-green, green, blue, black and peach spheres, respectively.

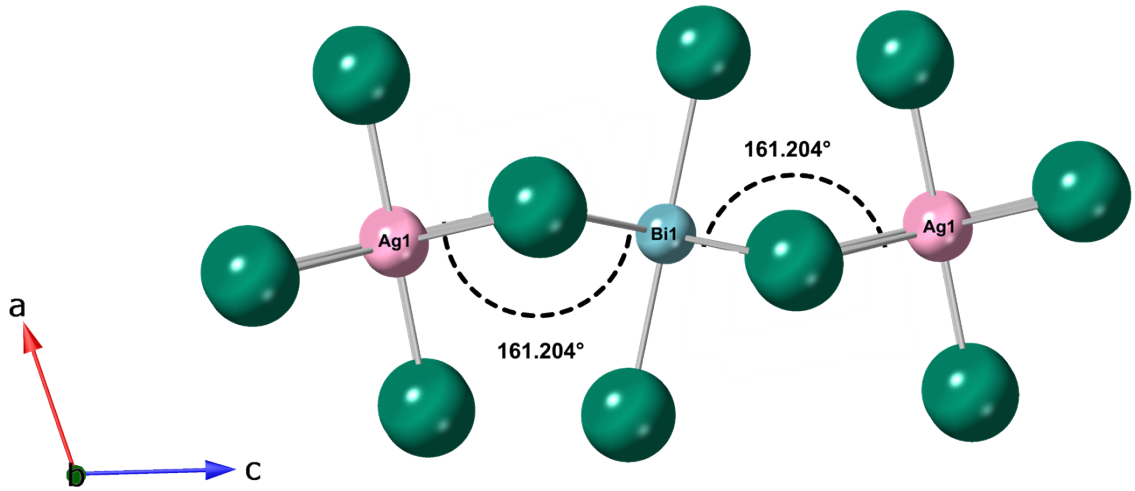

Fig. S10 The bridging Ag-Br-Bi and Bi-Br-Ag angles within the inorganic layers the in-plane direction shows reduced tilting at 400 K. Silver, bismuth, bromine are denoted by pink, bluish-green and green spheres, respectively.

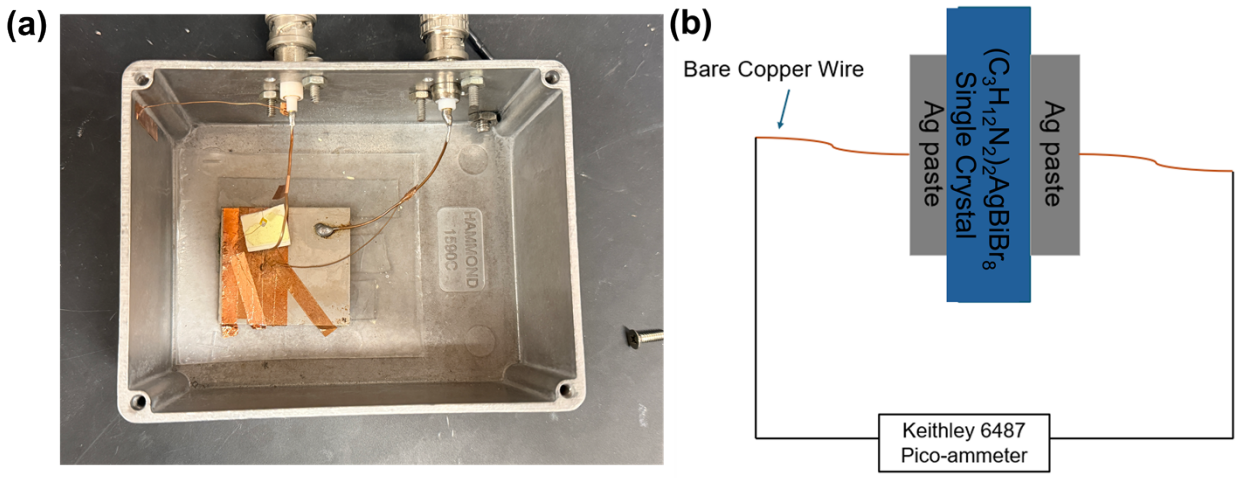

Fig. S11 (a) Set-up used for electrical measurements. (b) Schematic depiction of fabricated prototype detector based on single crystal of $(C_3H_{12}N_2)_2AgBiBr_8$.

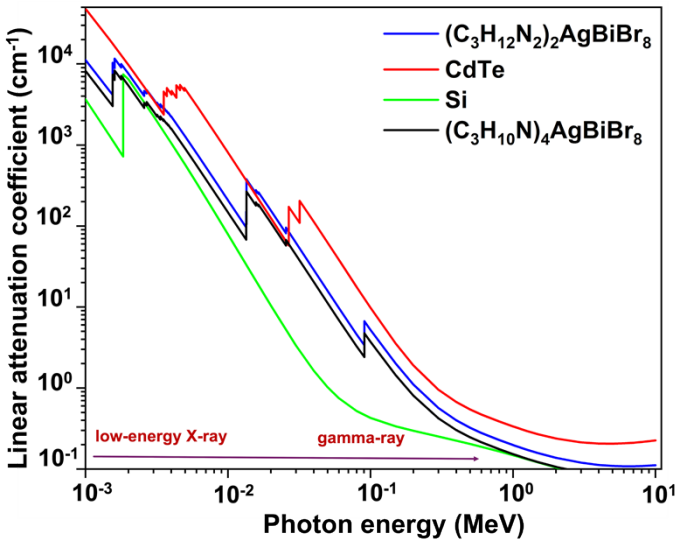

Fig. S12 Photon attenuation capability comparison plot for $(C_3H_{12}N_2)_2AgBiBr_8$, CdTe, Si and $(C_3H_{10}N)_4AgBiBr_8$ against soft low-energy X-rays and high-energy gamma rays.

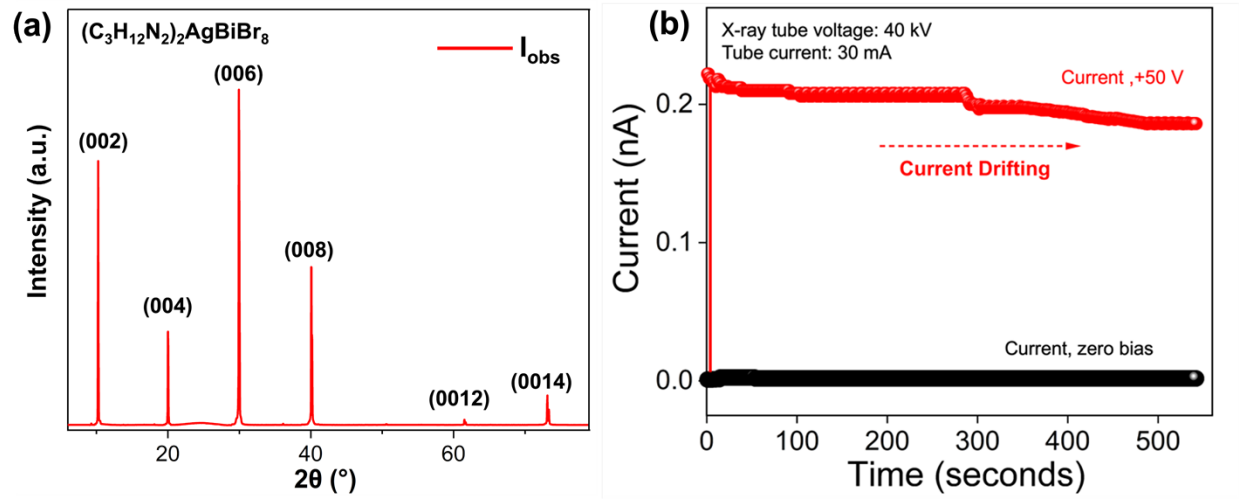

Fig. S13 (a) An indexed room temperature PXRD pattern of a single crystal of $(C_3H_{12}N_2)_2AgBiBr_8$ used for characterization of X-ray detection properties. (b) Long-term detector operational stability testing under continuous X-ray irradiation for ten minutes.